

Characterization of Silica–Titania Mixed Oxides

C. U. INGEMAR ODENBRAND, S. LARS T. ANDERSSON, LARS A. H. ANDERSSON,
 JAN G. M. BRANDIN, AND GUIDO BUSCA*

*Department of Chemical Technology, Chemical Center, Lund University, Institute of Science and Technology, P.O. Box 124, S-221 00 Lund, Sweden, and *Istituto di Chimica, Facoltà di Ingegneria, Università di Genova, Piazzale Kennedy, 16129 Genoa, Italy*

Received September 8, 1989; revised May 9, 1990

A series of coprecipitated silica–titanias containing between 0 and 100 mol% titania were characterized by various methods. These materials are often used as supports for catalysts in the reduction of NO_x and are shown to be micro-, meso-, and macroporous. All textural quantities decrease with the addition of TiO₂ to SiO₂. The macroporosity, of vital importance in the highly diffusion-controlled NO_x reduction, reaches a maximum value at 50 mol% TiO₂. X-ray diffraction, FT-IR, and XPS studies showed that the materials, calcined at 723 K, consisted of a SiO₂–TiO₂ glass phase, an amorphous silica phase, and an anatase phase. At 10 mol% TiO₂, rutile was observed, by XRD, in addition to anatase. XPS data indicate the presence of a TiO₂ phase in all Ti-containing samples, a SiO₂ phase at and below 50 mol% TiO₂, and a SiO₂–TiO₂ phase at and above 75 mol% TiO₂. The quantitative XPS analysis indicates a heterogeneous distribution of phases with an increased surface concentration of Si phases. Similar results were obtained by the FT-IR studies, which additionally indicate the presence of surface free silanol groups in all samples and detect tetrahedrally substituted Ti⁴⁺ in the SiO₂ phase. © 1990 Academic Press, Inc.

INTRODUCTION

Silica–titania mixed oxides are interesting materials from many points of view. In the glassy state, they may constitute materials having zero or negative thermal expansion (1, 2). Titanium can enter in small amounts into the framework of crystalline silicalite, producing titanium silicalite (3, 4), a very interesting new catalytic material. The surface properties of silica-supported titanias have been the object of several recent studies in view of the use of these solids as supports for metal catalysts (5–8). Mixed silica–titanias are very acidic materials (9) and a theory for the creation of acidic centers in them has been presented (10). They have also been used as acidic catalysts (11) and as supports for chromia-based ethylene polymerization catalysts (12). In recent years silica–titanias have been proposed as optimal supports for vanadia-based catalysts for catalytic reduction of NO_x (13–17).

Mixed silica–titanias obtained by different methods have been reported and characterized recently (18). Materials obtained by

coprecipitation from a solution of the two chlorides were found to be amorphous after calcination at 773 K even when the TiO₂ molar content is 75%, while gels prepared from the two alkoxides after calcination at 873 K segregate titania already when the molar amount of TiO₂ was 10% (17). These materials are used for “denoxing” catalysts because of the increased surface area, the increased temperature stability, and the material strength obtained compared with that when titania alone is used.

To increase knowledge on the effect of the catalyst–support interaction in the NO_x reduction it is important to characterize the support material carefully. The present paper reports the preparation and bulk characterization of coprecipitated silica–titanias as well as FT-IR and XPS studies of their surface structure.

METHODS

Preparation of SiO₂–TiO₂ Mixed Oxides

The mixed oxides of SiO₂ and TiO₂ were prepared by a homogeneous precipitation

procedure developed by Shikada *et al.* (13). The chemicals used were $\text{Na}_2\text{SiO}_3 \cdot 5\text{H}_2\text{O}$ (purum, Roth), TiCl_4 (R.G. 99.5%, Riedel-de-Haen), urea (R.G. 99.5%, Riedel-de-Haen), concentrated HCl (R.G. 37%, Merck), and distilled deionized water. The amounts of $\text{Na}_2\text{SiO}_3 \cdot 5\text{H}_2\text{O}$ and TiCl_4 were varied to obtain mixed oxides with TiO_2 content of 0 to 100 mol%. The sodium silicate was melted in a beaker and diluted with boiling water. The mixture was heated further on a water bath until a clear solution was obtained. This step was necessary to avoid premature gelation at later stages in the preparation procedure. After cooling to 273 K concentrated HCl was added rapidly under vigorous agitation to a pH of 1. A solution of Ti^{4+} in concentrated HCl was prepared simultaneously. A dropwise addition of TiCl_4 to the HCl at 273 K produced a yellow solution and a sticky mass of titanium hydroxychlorides. This substance was dissolved by addition of very small amounts of water (273 K). The two solutions were then mixed and urea was added. The temperature was increased to 363 K. During the heating period urea is decomposed slowly, yielding NH_3 and CO_2 . The ammonia dissolves rapidly in the aqueous phase, producing NH_4^+ and OH^- . The resulting homogeneously produced hydroxide ion gels/precipitates the mixed hydroxides of Si and Ti. This process requires several hours to go to completion and is continued until a final pH of 7 is reached. About 100 g of the gel was then washed by decantation with at least nine portions of water (1500 cm^3 each) or until no chloride ions could be detected by the AgNO_3 test. Drying was performed overnight at 393 K. Calcination was performed in several batches, each of about 10 g, in porcelain vessels under a stream of $10 \text{ cm}^3/\text{min}$ of dry (H_2SO_4) air. The temperature of the oven was increased at 10 K min^{-1} and the calcination was continued for 1 h at 723 K. Cooling was performed for another half-hour under the same atmosphere. The oxides were then stored in closed vessels

before use. Calcination was also performed in an oven at 1425 K for 2 h.

Characterization

The mixed oxides were characterized, after degassing at 620 K for 12 hr to a final pressure of 0.9 mPa, by N_2 -adsorption techniques in a gravimetric apparatus as described before (14). In addition to total BET surface area, pore volume, and pore size distribution, the micropore volume was determined using the Dubinin method (19). Hg porosimetry was used as a complementary method.

A Philips PW 1710 powder diffraction unit equipped with a PW 1050 wide-angle goniometer and a LiF monochromator was used to obtain X-ray diffraction spectra. Finely ground samples were scanned at a speed of 0.6° per minute over the diffraction angle range 5° to 60° . Peaks were identified by comparison with standard diffraction data (20). The average crystallite size (D) of SiO_2 and TiO_2 was calculated from the Scherrer equation: $D = k\lambda/[B^2 - b^2]^{1/2} \cos \Theta$ (21). The measured peakwidths at half-height (B) and the diffraction angle (Θ), both in radians, were used along with experimentally determined instrumental broadenings (b), to calculate the crystallite size. The value of the Scherrer constant (k) used was 0.90 and the wavelength of the radiation (λ) was 0.15418 nm. The reflection from the (101) plane was used for anatase [$\text{TiO}_2(\text{a})$]. Cristobalite [$\text{SiO}_2(\text{c})$] size was determined from a peak obtained at a d value of around 0.405 nm.

FT-IR spectra were recorded using a Nicolet 5ZDX spectrometer. The powders were pressed into self-supporting disks, treated in air in the IR cell at 635 K for 1 h, and evacuated for 1 h at 635, 790, or 1070 K.

XPS studies were performed on a Kratos XSAM 800 instrument. A Mg anode (1253.6 eV) was used. The slit width was set at 40° and the analyzer was operated at 40-eV pass energy and at high magnification. Charging effects were corrected for by adjusting the

TABLE 1
Characteristics of Silica-Titania Samples

Sample	TiO ₂ content (mol%)	S _{BET} (m ² /g)	Volume (cm ³ /g)		
			V _{mi}	V _{me}	V _{ma}
A	0.0	342	0.100	0.728	0.016
B	0.5	386	0.132	0.818	0.017
C	10.0	327	0.114	0.697	0.049
D	25.0	311	0.108	0.563	0.026
E	50.0	268	0.092	0.446	0.078
F	50.0	235	0.081	0.402	0.066
G	75.0	234	0.080	0.297	0.077
H	90.0	253	0.083	0.505	0.025
I	99.5	132	0.043	0.354	0.017
K	100.0	122	0.041	0.339	0.003

main C 1s peak to a position at 285.0 eV. Analysis of the spectra were performed with the DS 800 data system. Sensitivity factors used in the quantitative analysis were O 1s 0.66, C 1s 0.25, and Na KLL 2.30 as supplied by Kratos. The factors for Si 2p and Ti 2p were obtained by calibration with SiO₂ and TiO₂ and were Si 2p 0.134 and Ti 2p 1.304.

RESULTS

Textural Characteristics

Some of the structural characteristics of the materials determined by N₂ adsorption and Hg porosimetry are collected in Table 1. Surface area (S_{BET}), micropore volume (V_{mi}), and mesopore volume (V_{me}) all decreased slowly with the TiO₂ content. For samples containing 99.5 mol% or more TiO₂ the surface area and the micropore volume decrease drastically. Micropore volumes are quite large in samples with large amounts of silica, and in sample B, V_{mi} was as much as 75% of the values typical of zeolites such as mordenite (19).

When silica is precipitated at pH 7 the surface area obtained is around 400 m²/g and the pore volume around 0.7 cm³/g (22). Comparison with sample A above shows excellent agreement in the pore volume. The

volume of the macropores (V_{ma}) with pore diameters of 45–1600 nm was determined by Hg porosimetry. Low values were obtained in the pure samples A and K and high values in the mixed oxides, especially at 50 mol% TiO₂ (0.08 cm³/g). Some of the mercury is not released from the pores when the pressure is returned to atmospheric during the extrusion process. The extrusion curve always lies above the intrusion curve. The intrusion curve measures the throats to larger cavities behind them in materials composed of spherical particles. These cavities are measured by the extrusion process and in all samples are large (16–50 nm) compared with the throats (8–17 nm). The width of the throats does not vary much with the amount of TiO₂ though somewhat higher values are obtained for the mixed oxides than for the pure components. The cavities are around 20 nm for SiO₂ (A), 30 nm for samples C–H, and 43 nm for TiO₂ (K). The structure of the mixed oxides is thus shown to be micro-, meso-, and macroporous.

X-Ray Diffraction

Calcination of samples A and B at 723 K produced materials which had only one broad structure in the XRD spectra, suggesting largely amorphous silica. The peak obtained is at 0.405 nm which coincides with the strongest reflection for α -cristobalite [SiO₂ (α -c)]. As the amount of TiO₂ is increased to 10 mol% in sample C peaks from both anatase (0.353, 0.238, and 0.190 nm) and rutile (0.328, 0.250, and 0.169 nm) are present. At 25 mol% TiO₂, silica is still evident in the spectra though partly hidden by the anatase peak at 0.353 nm. At TiO₂ contents of 50 mol% and higher, the material becomes slightly more crystalline and only anatase is observed in the spectra.

It is assumed that the material contains microcrystalline cristobalite, the line-broadening analysis indicates a crystallite size of around 1.1 nm. The size of the anatase crystallites changes with the composition. The size determined from the peak for the (101)

TABLE 2

X-Ray Diffraction Analysis of the Anatase Phase in Mixed SiO_2 - TiO_2 Oxides Containing 99.5 mol% or More TiO_2

Literature value		Experimental value				
Plane	Anatase	Sample K (100 mol% TiO_2)		Sample I (99.5 mol% TiO_2)		
(hkl)	d value	Intensity	d value	Intensity	d value	Intensity
101	3.52	100	3.52	100	3.53	100
103	2.431	10	2.474	22		
004	2.378	20	2.377	23	2.380	30
112	2.332	10				
200	1.892	35	1.894	27	1.897	30
105	1.699	20	1.692	23	1.701	24
211	1.667	20	1.660	22	1.672	20
204	1.481	14	1.482	14		
116	1.364	6	1.362	7		
220	1.338	6	1.338	6		
215	1.265	10	1.265	9		

plane increases from 3.6 to 5.3 nm from 10 to 90 mol% TiO_2 . At 99.5 and 100% TiO_2 the respective values are 10.3 and 9.4 nm. It is thus shown that the only crystalline phase present in the low-temperature calcined samples is anatase. No intermediate compounds could be identified by X-ray diffraction. Sample K (100 mol% TiO_2) has an X-ray diffraction pattern very close to the one described in the literature for $\text{TiO}_2(\text{a})$ (20). Addition of only 0.5 mol% SiO_2 to TiO_2 yields a material that is much less crystalline and has only the five major peaks of anatase visible (see Table 2). For samples A-H the particle size obtained from S_{BET} and ρ_s is around 8 nm and for samples I-K it increases to 13 nm.

Calcination at 1425 K produced sintered materials with surface areas around 0.6 m²/g, shown by XRD to consist of α -cristobalite. The diffraction patterns of samples A and B show all the major peaks of $\text{SiO}_2(\alpha\text{-c})$ and no peaks from TiO_2 . Samples C to F consist of $\text{SiO}_2(\alpha\text{-c})$, $\text{TiO}_2(\text{a})$, and $\text{TiO}_2(\text{r})$, rutile, in varying amounts. Samples G to I contained $\text{TiO}_2(\text{a})$ and $\text{TiO}_2(\text{r})$, and sample K the rutile only. No other new compounds could be identified in any sample. The inten-

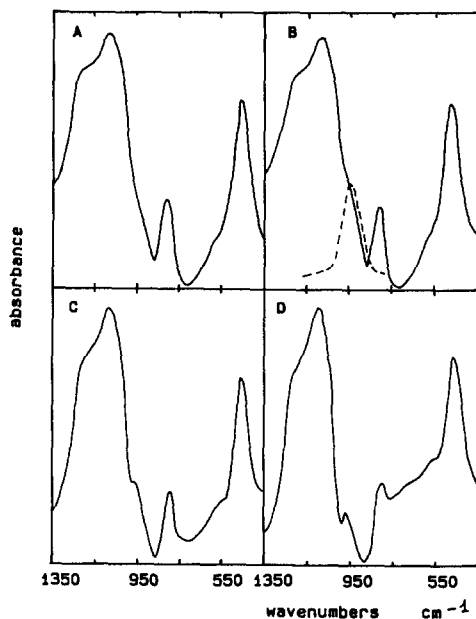


FIG. 1. FT-IR spectra (KBr pressed disks) of samples A to D. The broken line represents the B-A difference spectrum.

sity of the cristobalite peak decreased rapidly with increasing additions of TiO_2 . At 10 mol% TiO_2 it was only about 30% of the value for SiO_2 alone. Crystallite size decreased simultaneously from 57 to 38 nm. This change in size should not result in such a large decrease in intensity. An increase in d value from 4.05 in sample A to 4.10 in sample F was also observed. This is in line with the effects of insertion of the larger Ti^{4+} ion into the silica lattice. The conclusion is that a new amorphous SiO_2 - TiO_2 glass phase is formed.

Infrared Studies

IR spectra in the skeletal vibration range (KBr pressed disks). The spectrum of sample A (Fig. 1) is similar to that of other amorphous silica samples, such as Cab-O-Sil from Cabot and Aerosil from Degussa. Three main absorptions are observed, generally assigned to the asymmetric and symmetric Si-O-Si stretchings and to the corre-

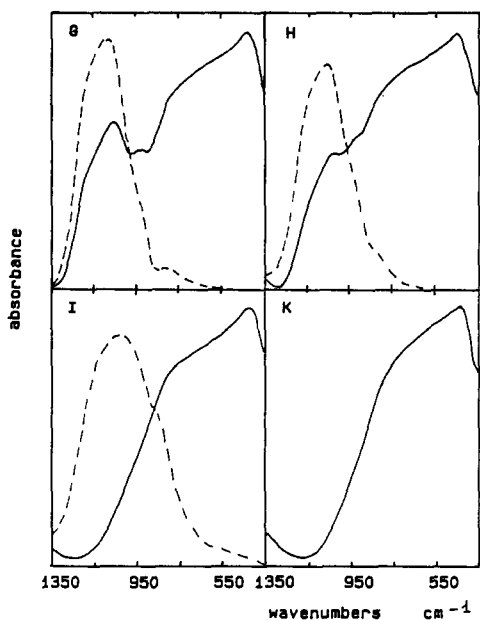


FIG. 2. FT-IR spectra (KBr pressed disks) of samples G, H, I, and K. The broken lines represent the spectra of samples G to H from which the K spectrum has been subtracted.

sponding deformation (23, 24). The main maximum corresponding to the first mode is observed by us at 1090 cm^{-1} with a well-resolved shoulder at 1230 cm^{-1} and other ones, almost unresolved at 1050 and 935 cm^{-1} . The symmetric mode is observed by us as a symmetric band near 810 cm^{-1} , while the deformation mode is detected as a main band at 465 cm^{-1} and a broad shoulder at 570 cm^{-1} . The spectrum of B is also very similar, but shows the shoulder near 940 cm^{-1} slightly more evident.

The ratio between the A and B spectra (broken line in Fig. 1, sample B) shows that the addition of $0.5\text{ mol}\%$ TiO_2 causes the appearance of a new band near 950 cm^{-1} . In the spectra of C and D this absorption appears as an individual weak maximum near 960 cm^{-1} , which is evident, although broader and shifting slightly downward (to near 940 cm^{-1}), also in the spectra of E, F, and G (Fig. 2). This band has already been

observed in the IR spectra of crystalline titanium silicalite (3, 25), as well as in both IR and Raman spectra of $\text{SiO}_2\text{-TiO}_2$ glasses (1, 2) and assigned to a Si-O-Ti asymmetric stretching.

In the spectra of samples C to F the spectrum of silica is still observable, but is progressively modified by a broad absorption growing in the region below 800 cm^{-1} . The characteristic shape of the complex band centered near 1100 cm^{-1} is still evident also in the G spectrum (Fig. 2), where a broadband having a shoulder near 750 cm^{-1} and the main maximum near 440 cm^{-1} is predominant. This band is that typical of TiO_2 anatase (26), reproduced almost exactly by the spectrum of K (Fig. 2). The spectra of I and H correspond to that of K on which a broadband is superimposed, centered at 1030 and 1070 cm^{-1} , respectively. This band can be seen in the broken lines in Fig. 1, obtained by subtraction of spectrum K from spectra G, H, and I; this band, due to Si-O stretchings, does not correspond exactly to that of silica. Another structure must then be formed on the low-silica-content samples.

IR spectra of the pure powder disks. The IR spectra of some samples prepared by pressing the pure powders without any binding material and further activating *in vacuo* at 790 K are shown in Fig. 3. As is usual these samples show a cutoff on the low-frequency side where the skeletal vibrations fall. This limit is near 1300 cm^{-1} for pure silica and the high-silica-content samples (up to G) while for pure titania it is observed near 1000 cm^{-1} due to the much lower frequencies for the Ti-O stretching modes compared with those of Si-O (see Figs. 1 and 2). In the spectrum of H (shown in Fig. 3) immediately above the cutoff limit we may observe the $\nu(\text{Si-O})$ band. It should correspond to the one discussed above for KBr disks. However, under these conditions the band is significantly shifted upward and is sensitive to the evacuation treatment. In fact it is detected near 1200 cm^{-1} after

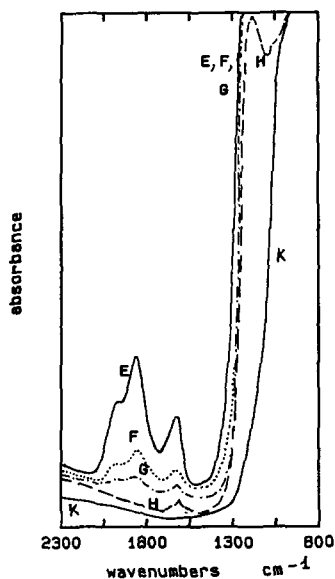


FIG. 3. FT-IR spectra of the pure powder samples evacuated at 790 K.

activation at 790 K and near 1220 cm^{-1} after activation at 1073 K. This behavior is consistent with the idea that this band is predominantly due to the stretching of Si-O bonds exposed at the catalyst surface.

In the region $2000\text{--}1500\text{ cm}^{-1}$ the spectrum of pure silica shows a strong absorption triplet, due to overtone and combination vibrations of the skeletal vibrations (28, 29). These bands are observable and are very intense in the spectra of samples A to E, while they are much smaller in the spectra of samples F and G and are absent in those of samples H to K (Fig. 3). This confirms that bulk silica is not present when the nominal silica molar concentration is of the order of 10 mol% or below. If calcination of the high-titania-content samples is not carried out, bands in the region $1800\text{--}1000\text{ cm}^{-1}$ are observed. These bands disappear upon heating in oxygen. They are due to residual C-containing adsorbed species (carbonates or carboxylates) that burn away upon calcination.

Characterization of the surface hydroxy groups. The IR spectra of the activated sam-

ples show, sharp bands in the region $3800\text{--}3600\text{ cm}^{-1}$, which could be assigned to $\nu(\text{OH})$ of free surface hydroxy groups. The spectrum of sample A is the usual one for pure silica (28, 29) even in this respect. It shows a very sharp and perfectly symmetric band at 3748 cm^{-1} if activation is carried out at 1073 K (Fig. 4, sample A). If activation is carried out at 790 K it is slightly broader at 3746 cm^{-1} and has shoulders at 3830 cm^{-1} (weak) and 3640 cm^{-1} (intense). The low-frequency absorption is due to $\nu(\text{OH})$ of internal weakly H-bonded hydroxy groups (30), while the higher-frequency one (3830 cm^{-1}) has been assigned to the $\nu + \gamma$ combination of free hydroxy groups (31). The present data suggest that it is due to a combination vibration of internal (slightly H-bonded) hydroxy groups, whose stretching is at 3640 cm^{-1} . In fact both bands disappear by evacuation at 1073 K, when these internal hydroxyls condense and evolve H_2O .

The spectra in the $\nu(\text{OH})$ region of samples A to G are similar. The addition of titanium seems to increase only slightly the sta-

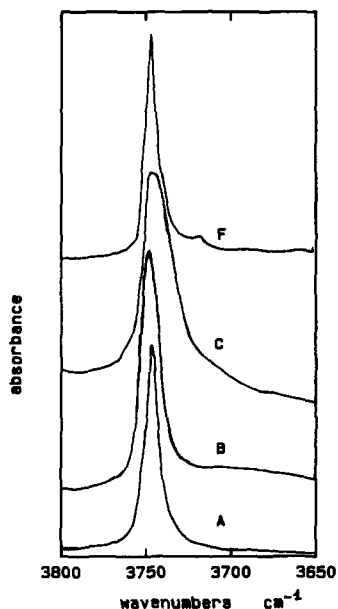


FIG. 4. FT-IR spectra in the $\nu(\text{OH})$ region of samples A, B, C, and F evacuated at 1073 K.

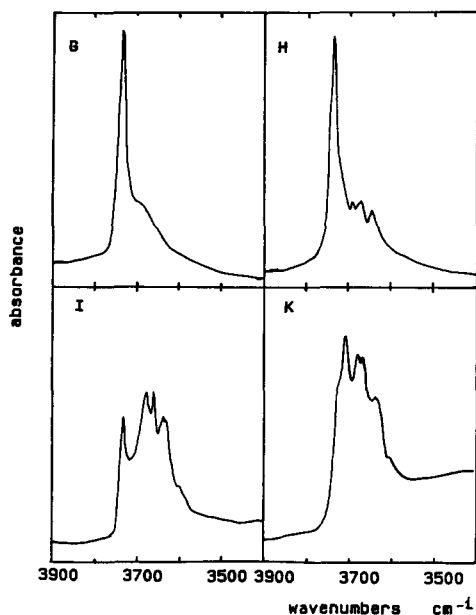


FIG. 5. FT-IR spectra in the $\nu(\text{OH})$ region of samples G, H, I, and K evacuated at 790 K.

bility of the species absorbing near 3640 cm^{-1} . In Fig. 4 the $\nu(\text{OH})$ bands observed for A, B, C, and F after evacuation at 1073 K are compared. These bands are significantly broadened in sample B and especially in samples C, D, and E (half-height width 19 cm^{-1} compared with 12 cm^{-1} for B and 10 cm^{-1} for A). At higher TiO_2 content it is again sharpened in samples F to I. The frequency in all these cases is near 3748 cm^{-1} .

When the nominal TiO_2 concentration rises to 90% (Fig. 5, sample H) the $\nu(\text{OH})$ band of free silanol groups is still very intense. However, its position is at a slightly but significantly lower frequency (3737 cm^{-1} after activation at 790 K, 3743 cm^{-1} after activation at 1073 K). After activation at 790 K (Fig. 5, sample H), on the low-frequency side of the silanol band, several components are resolved (3680 , 3670 , and 3640 cm^{-1}). In the spectrum of I these bands, located at the same positions, are predominant with respect to another sharp band observed at 3735 cm^{-1} , still evident and very probably also due to free silanol groups. The spec-

trum of the pure TiO_2 sample shows again bands at 3640 cm^{-1} (shoulder), 3670 , and 3680 cm^{-1} , together with a weak shoulder at 3610 cm^{-1} and the most intense band detected at 3710 cm^{-1} , having a shoulder at 3730 cm^{-1} . The spectrum looks very similar to that of other anatase samples (32).

Study of the adsorption of CO. From previous studies it is well known that CO interacts at room temperature (r.t.) with surface Ti cations on TiO_2 surfaces (32, 33) while it only H-bonds on silanol groups of silica very weakly (34). We have chosen CO as a probe molecule to test the presence and the nature of Ti sites on the surface of our materials. In Table 3 our assignments for the bands arising from adsorbed CO are summarized. The spectrum of CO adsorbed species on sample K (Fig. 6, sample K) is the usual one for anatase surfaces (32, 33). It is composed of two main absorption bands at 2187 cm^{-1} (strong) and 2206 cm^{-1} (weak). These bands have previously been assigned to carbonyl species on octahedrally coordinated Ti^{4+} cations having one and two coordinative unsaturations respectively (32, 35). By increasing the silica nominal content the spectrum is modified progressively in the following sense: (i) the absolute intensity of the band near $2185\text{--}2190 \text{ cm}^{-1}$ decreases progressively, due to the decrease in the amount of the adsorption sites; this band is still detectable, very weak, in sample C (Fig. 6) while it is not apparent in samples B and A; (ii) the relative intensity of the higher-

TABLE 3

Assignments of the Bands Arising from Adsorbed CO

Wavenumber (cm^{-1})	Structure
2225	$\text{O}_3\text{Ti}^{4+}\text{-CO}$
2206	$\text{O}_4\text{Ti}^{4+}\text{-CO}$
2188	$\text{O}_5\text{Ti}^{4+}\text{-CO}$
2130	$\text{O}_x\text{Ti}^{3+}\text{-CO}$
2110	$\text{O}_x\text{Ti}^{3+}\text{-CO}$

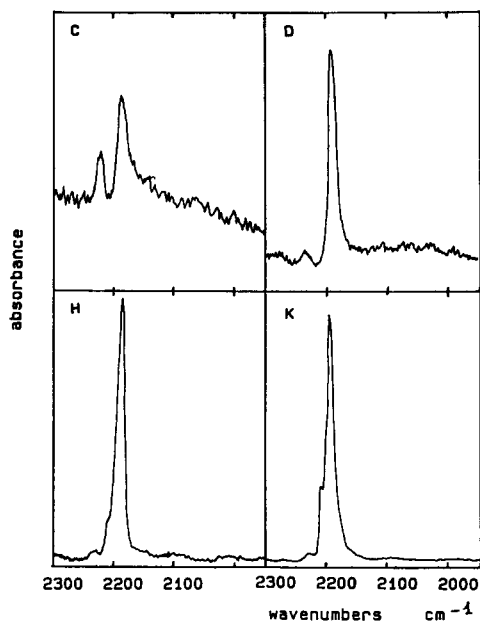


FIG. 6. FT-IR spectra of CO (100 Torr) adsorbed on samples C, D, H, and K activated at 790 K.

frequency component (2206 cm^{-1}) with respect to the lower-frequency one decreases and has disappeared in samples D (Fig. 6) and E (Fig. 7); (iii) a third band at 2225 cm^{-1} is evident, although weak, in sample C; this band is detectable on all samples from C to K, always very weak, its relative intensity with respect to the band near 2188 cm^{-1} being increased at higher silica contents. According to the variation of the relative intensity of this band in relation to the sample composition and to its frequency we assign it to carbonyl species on tetrahedral Ti^{4+} centers.

In Fig. 7 the changes in the spectra of adsorbed CO obtained by increasing the evacuation time at 790 K are exemplified for sample E. If evacuation is carried out for 3 h the bands discussed above decrease in intensity while two bands which are stable upon evacuation at r.t., unlike the previous ones, grow at 2133 and 2118 cm^{-1} . The positions of these bands below the frequency of gaseous CO (2143 cm^{-1}) indicate that the adsorption center contains d electrons that

cause π -type backbonding from the metal center to the antibonding orbitals of CO. According also to the thermal stabilities of these species we assign these bonds to carbonyl species on Ti^{3+} centers (32). For pure TiO_2 prolonged evacuation at 790 K causes loss of transmittance by the sample (36), certainly related to a partial surface reduction.

XPS Studies

Table 4 shows the core lines measured by XPS for the different SiO_2 - TiO_2 mixed oxides. By comparison with sample K (100 mol% TiO_2), which gave reference data for the Ti $2p_{3/2}$ binding energy (B.E.), it is seen that Ti is in all samples (B-K) present as Ti^{4+} and probably as the intact TiO_2 . A similar comparison for SiO_2 (sample A, 0 mol% TiO_2) shows that the Si $2s$ and Si $2p$ binding energies for samples A through F (0–50 mol% TiO_2) identify the presence of SiO_2 . At lower SiO_2 content, i.e., greater than 75 mol% TiO_2 in samples G–I, a definite decrease in the Si $2s$ and Si $2p$ binding energies is obtained. Generally, the Si $2p$ B.E. is highest for pure SiO_2 and much lower, around 102 eV, for various silicates (37). The low Si $2p$ B.E. of 102 eV for samples H

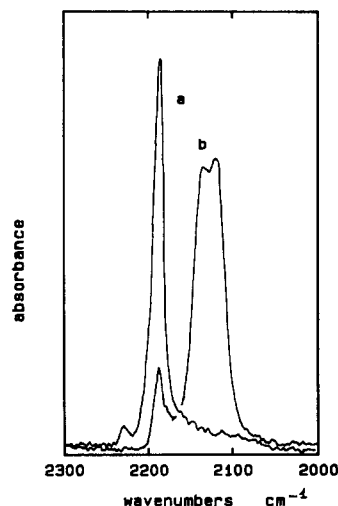


FIG. 7. FT-IR spectra of CO (100 Torr) adsorbed on sample E evacuated at 790 K for 1 hr (a) and 3 h (b).

TABLE 4

Core Electron Binding Energies^a (eV) and FWHM^b for SiO₂-TiO₂ Mixed Oxides

Sample	mol% TiO ₂	O 1s ^c	Si 2s	Si 2p	Ti 2p _{3/2}
A	0.0	533.1 (2.3)	—	154.8 (3.0)	103.7 (2.4)
B	0.5	533.0 (2.3)	—	154.7 (2.9)	103.6 (2.3)
C	10.0	533.0 (2.2)	—	154.6 (2.9)	103.7 (2.3)
D	25.0	533.1 (2.4)	530.2 (1.7)	154.8 (3.0)	103.7 (2.3)
E	50.0	533.0 (2.7)	530.2 (1.6)	154.7 (3.0)	103.6 (2.5)
F	50.0	533.1 (2.5)	530.3 (1.6)	154.8 (3.0)	103.8 (2.4)
G	75.0	532.5 (2.3)	530.3 (1.6)	154.1 (2.7)	102.9 (2.3)
H	90.0	532.3 (2.2)	530.3 (1.7)	153.1 (2.1)	102.0 (2.0)
I	99.5	532.3 (2.5)	530.3 (1.6)	153.2 (1.6)	101.9 (1.4)
K	100.0	532.3 (2.6)	530.4 (1.5)	—	— (1.4)

^a Charging corrected for by adjusting the main C 1s line to 285.0 eV.

^b Within parentheses.

^c Fitted with Gaussian components.

and I indicates formation of some titanium silicate. The intermediate value, 102.9 eV for sample G, indicates a different composition, perhaps a TiO₂-SiO₂ glass with a low Ti content. This spectrum cannot be synthesized from one component at 103.7 eV (spectra A-F, Fig. 8) and another at 102 eV (spectra H-I, Fig. 8). Spectra E and F (Fig. 8) are slightly asymmetric toward low B.E. and a comparison with spectra A-D suggests that the former contains a contribution of about 5% from a Si 2p component at around 102-103 eV, similar to the one at 102.9 eV for sample G. It therefore seems that going from 75 to 50 mol% TiO₂ results in a strong reduction in the silicate concentration as detected by XPS.

The above conclusions are supported by the O 1s spectra. Table 4 shows the B.E. for two Gaussian components fitted to the O 1s peak. For pure SiO₂ (sample A) a B.E. of 533.1 eV is obtained for O 1s. This component is seen in all samples up to 50 mol% TiO₂. From 25 mol% TiO₂ and upward, a second O 1s component is appearing at 530.2

eV, which is characteristic of O 1s in TiO₂. At a composition of 75 mol% TiO₂ and above, however, the high-B.E. O 1s component (533.1 eV) shifts to a lower value of 532.5 and finally 532.3 eV. This lower O 1s B.E. also identifies the formation of silicates, as was the case in the Si 2p peak. The resolution of the O 1s spectra into two Gaussian components could not be done with a perfect fit (see Fig. 9, sample A). The reason is basically that the natural lineshape differs from the assumed Gaussian. For SiO₂ the O 1s lineshape is symmetrical, but not so for TiO₂, due to the difference in the density of states and due to a contribution from surface carbonate and hydroxyl groups. Therefore the natural curve form of the O 1s line for the two unmixed components, SiO₂ and TiO₂, was applied in curve fitting for the O 1s line of all the samples. The result is shown in Figs. 9B-H. Com-

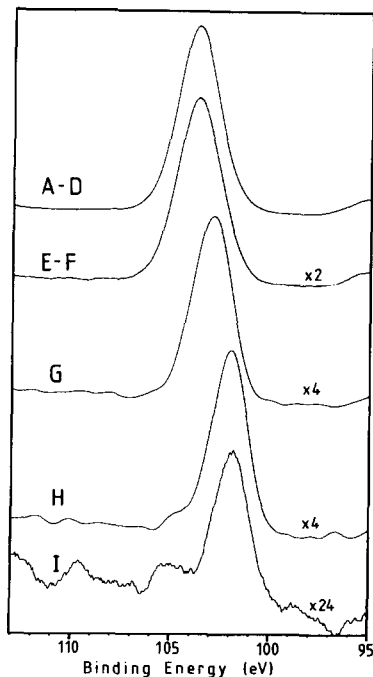


FIG. 8. Si 2p spectra for various SiO₂-TiO₂ mixed oxides. Notations follow sample notation. Spectra A-H were treated with a 29-point and spectrum I with a 61-point quadratic smoothing (step interval 0.05 eV).

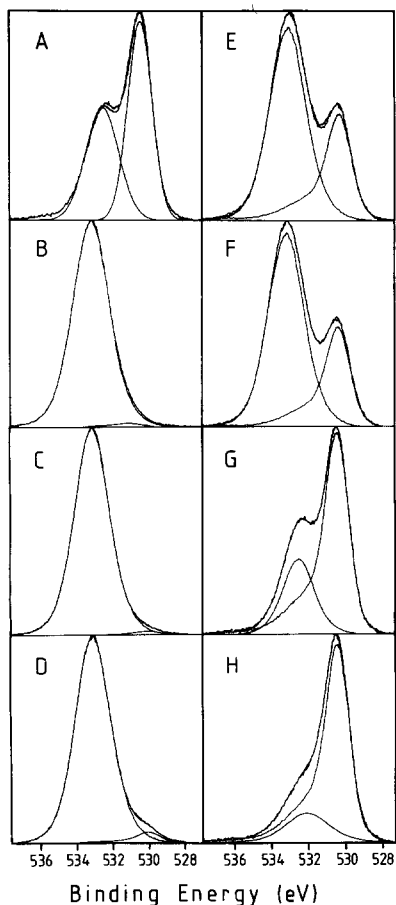


FIG. 9. O 1s spectra for various SiO₂-TiO₂ mixed oxides fitted with two Gaussian components (A) or with the natural curve profile measured for SiO₂ and TiO₂ (B-E). Compositions in mol% TiO₂. (A) 75%, (B) 0%, C-H follow sample notation.

pared with the result when Gaussian shapes are used, the fit is very good.

Following this result, quantification of the XPS data was performed. The mol% TiO₂ was calculated in two different ways. The first, and most evident, was to calculate it from the Si 2*p* and Ti 2*p* peak areas as Ti/(Ti + Si) with sensitivity factors measured on TiO₂ and SiO₂. The second method was to calculate it from the contribution of the two components in the O 1s spectra of Fig. 9. As shown in Fig. 10 both methods give similar results. It is quite clear that all samples give lower Ti concentrations than ex-

pected. As was shown above, the samples are mixtures of at least two phases. A TiO₂ phase appears in all Ti-containing samples. The other is a SiO₂ phase at high, and a Ti silicate at low Si contents. If the Si-containing phases are of a much higher dispersion than the TiO₂ phase, a pure geometrical packing effect would give a higher contribution of these than of the TiO₂ phase. It is also seen that the effect is strongest at low Ti concentrations.

Several samples were observed by XPS to be contaminated by sodium and carbonate. The Na KLL Auger peak appeared only at higher concentrations of silica, with the exception of sample F. (Na/(Si + Ti) atom ratios decreased from 0.01 to 0.0007 going from sample A to C. The origin of sodium is the precursor sodium silicate and it is indeed difficult to wash these materials free from sodium. The C 1s lines for samples E-K gave spectra containing a specific structure at 289 eV for carboxylate and at 286.5 eV for possibly carbonyl or other oxygen-bonded carbon species. It appears as if the carboxylate is associated with the presence of TiO₂. The contribution from carboxylate in the O 1s spectra is estimated to be 5%, and

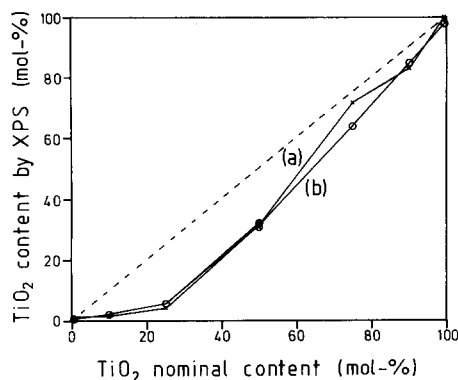


FIG. 10. Atom percentage Ti [Ti/(Si + Ti)] measured by XPS versus the bulk composition. (a) Calculated as O(Ti)/[O(Si) + O(Ti)] from the O 1s components obtained by fitting the natural curve form of O 1s for SiO₂ and TiO₂ to the O 1s spectrum. (b) Calculated from Ti 2*p* and Si 2*p* after calibration with SiO₂ and TiO₂ relative to O 1s.

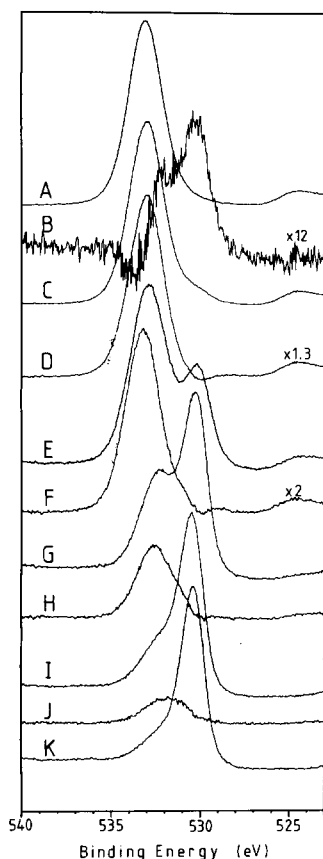


FIG. 11. O 1s difference spectra for some mixed SiO₂-TiO₂ oxides. (A) 10 mol% TiO₂, (B) 25 mol% TiO₂ - 10 mol% TiO₂, (C) 25 mol% TiO₂, (D) 25 mol% TiO₂ - 50 mol% TiO₂, (E) 50 mol% TiO₂, (F) 50 mol% TiO₂ - 75 mol% TiO₂, (G) 75 mol% TiO₂, (H) 75 mol% TiO₂ - 100 mol% TiO₂, (I) 90 mol% TiO₂, (J) 90 mol% TiO₂ - 100 mol% TiO₂, (K) 100 mol% TiO₂.

probably gives a contribution to the structure seen at 532 eV in the O 1s spectra for TiO₂ (Fig. 9).

Figure 11 shows some O 1s difference spectra. The difference spectrum between O 1s for 90 and 100 mol% TiO₂ gives a symmetric peak at 531.8 eV due to titanium silicate (spectrum J). The difference spectrum between O 1s for 75 and 100 mol% TiO₂ shows an asymmetric peak suggesting the presence of one component at 533 eV and one at 531.8 eV corresponding to SiO₂ and the titanium silicate, respectively (spec-

trum H). The difference spectrum between O 1s for 50 and 75 mol% TiO₂ (spectrum F) also suggests the presence of two components. The SiO₂ component is progressively increasing in importance and the second component is not seen in the difference spectrum for 25 and 50 mol% TiO₂ (spectrum D). The difference spectrum between 25 and 10 mol% TiO₂ (spectrum B), where the SiO₂ component has been subtracted, shows the presence of two components, one around 530 eV for TiO₂ and another around 532 eV. The second may be due to titanium silicate or to dispersed Ti-O-Si species.

DISCUSSION

The IR data for the skeletal vibrations and the XPS data are in agreement with the XRD data indicating that TiO₂ is in the form of anatase at TiO₂ of 10 mol% and higher content. This is also consistent with the spectra of adsorbed CO, which are typical of CO on anatase (32, 33). Also, the spectrum of the surface hydroxy groups agrees with that for anatase samples. However, this spectrum is perturbed strongly when even small amounts of silica are present and at 0.5 mol% SiO₂ (sample I) a sharp $\nu(\text{OH})$ band at 3736 cm⁻¹ is observed. The shape and position of this band suggest its assignment to $\nu(\text{OH})$ of surface free silanol groups. It seems relevant that the band of surface silanols shifts down remarkably in the high-titania-content samples. In these samples, and particularly in sample H, the presence of surface Si-O bonds, perturbed upon adsorption-desorption cycles, is also evident from the detection of a surface-sensitive $\nu(\text{Si-O})$ band. The presence of SiO_x species (different from bulk silica) on the surface of the high-TiO₂-content samples is then very likely.

The $\nu(\text{OH})$ band at 3710 cm⁻¹, which is the strongest $\nu(\text{OH})$ in the spectrum of sample K, disappears completely in the spectrum of sample I, while the band of CO adsorbed on the doubly coordinatively unsaturated cations (2206 cm⁻¹) also decreases remarkably. According to the argu-

ments of Knözinger and Ratnasamy (38) the highest-frequency $\nu(\text{OH})$ band is expected to be due to hydroxy groups bonded to the lowest-coordination cations. It seems then reasonable to conclude that in the structure of the high-titania-content samples silicon species tend to substitute titanium cations in the low-coordination surface defects. This would result in a surface enrichment of silicon oxide species in the form of isolated SiO_4 tetrahedra or of small Si_xO_y "clusters", with the appearance of silanol groups having a lower $\nu(\text{OH})$ than on pure silica and characteristic $\nu(\text{Si-O})$ bands, as well as with the disappearance of low-coordination TiOH groups and exposed Ti^{4+} cations. The present data support the previous idea that sharp bands near 3735 cm^{-1} present in the spectra of activated titania preparations are due to silica impurities (32).

These results are confirmed by XPS data, which show that bulk silica is present in samples A to F (silica content 100 to 50 mol%), while the features of anatase are detected in all Ti-containing samples. The XRD studies revealed that anatase is present in all samples with a titania content higher than 10 mol%. Moreover, XPS showed that species different from SiO_2 and anatase are present in samples G, H, and I (nominal SiO_2 content 25, 10, and 0.5 mol%). These species are characterized by a Si $2p$ B.E. between 102.9 and 101.9 eV and an O $1s$ B.E. of about 532 eV. These features are similar to those of metal silicates (37) and have been assigned to a titanium silicate species. The fact that the Si $2p$ B.E. for the silicate phase varies when going from 0.5 to 25 mol% SiO_2 shows that its composition is shifting. The low B.E. at 0.5 and 10 mol% SiO_2 indicates a strong interaction with Ti^{4+} , which is the case for both titanium silicate and silicon oxide species bonded to the TiO_2 surface as suggested by IR results. The quantitative XPS analysis shows indeed a much higher Si/Ti ratio than expected. At 25 mol% SiO_2 , however, the Si $2p$ B.E. of 102.9 eV, intermediate between that for SiO_2 and that for titanium

silicate, suggests a different silicate composition. The peak shape identifies a single component only. In the same composition range, less than 25 mol% SiO_2 , FT-IR studies show that the asymmetric Si-O-Si stretching bonds are strongly modified indicating a different structure.

The main features of the high-silica-content samples give information on the state of titanium centers on these materials. The formation of an IR band near 950 cm^{-1} is a clear indication of the insertion of Ti^{4+} in tetrahedral sites into the silica framework, as on silica-titania glasses (1, 2) and titanium silicalite (3, 25). This is also supported by the detection of a band due to adsorbed CO at 2225 cm^{-1} . This band is very likely to be due to CO on coordinatively unsaturated tetrahedral Ti^{4+} cations. It is then reasonable to conclude that the low-titania-content samples contain an amorphous solid solution where titanium substitutes a small amount of silicon in tetrahedral coordination. The lack of any larger shifts in the Ti $2p_{3/2}$ B.E. by XPS is not contradictory since variations in the cation in titanates result only in small shifts of a few tenths of an electron volt (39).

At TiO_2 contents of 10 mol% and higher, anatase is present according to the XRD analysis. The IR studies showed a broad peak around 800 cm^{-1} assigned to anatase and it gives a contribution in the spectra already at 10 mol% TiO_2 (sample C). Thus a substantial part of the titanium is present as anatase, which is also in agreement with the Ti $2p_{3/2}$ B.E. measured by XPS.

XPS analysis is also very useful in detecting the presence of impurities on the surface of the mixed oxides. The presence of C-containing species (carboxylates) is observed both by IR and by XPS in samples of high TiO_2 content. This is explained by the higher ionicity of titania compared to silica and consequently its higher tendency to adsorb this type of species and to retain them. Conversely, significant amounts of sodium are present in samples of high SiO_2 content in line with the higher covalency of

silica and the higher acidity of its silanol groups which may be partially exchanged by Na⁺.

ACKNOWLEDGMENTS

The authors are grateful for the professional skill in using XRD and gravimetric adsorption equipment provided by Mrs. Birgitta Svensson. This study was supported by the National Energy Administration of Sweden.

REFERENCES

- Görlich, E., Blaszczyk, K., Stoch, A., and Sieminska, G., *Mater. Chem.* **5**, 289 (1980).
- Brest, M. F., and Condrate, R. A., *J. Mater. Sci. Lett.* **4**, 994 (1985).
- Taramasso, M., Perego, G., and Notari, B., U.S. Patent 4.410.501.
- Bellussi, B., Perego, G., Esposito, A., Corno, C., and Buonomo, F., in "Proceedings, VI Italian Congress on Catalysis, Cagliari, 1986," p. 423.
- Reichmann, M. G., and Bell, A. T., *Appl. Catal.* **32**, 315 (1987).
- Reichmann, M. G., and Bell, A. T., *Langmuir* **3**, 311 (1987).
- Kataoka, T., and Dumesic, J. A., *J. Catal.* **112**, 66 (1988).
- Fernandez, A., Leyrer, J., Gonzalez-Elipse, A. R., Munuera, G., and Knözinger, H., *J. Catal.* **112**, 489 (1988).
- Shibata, K., Kiyoura, T., Kitagawa, T., Sumiyoshi, T., and Tanabe, K., *Bull. Chem. Soc. Japan* **46**, 2985 (1973).
- Tanabe, K., in "Catalysis, Science and Technology," (J. R. Anderson and M. Boudart, Eds.), Vol. 2, p. 231. Springer-Verlag, Berlin, 1981.
- Niwa, M., Sago, M., Ando, H., and Murakami, Y., *J. Catal.* **69**, 69 (1981).
- McDaniel, M. P., and Welch, M. B., *J. Catal.* **82**, 98 (1983).
- Shikada, T., Fujimoto, K., Kunugi, T., and Tomimaga, H., *Ind. Eng. Chem. Prod. Res. Dev.* **20**, 91 (1981).
- Odenbrand, C. U. I., Lundin, S. T., and Anderson, L. A. H., *Appl. Catal.* **18**, 335 (1985).
- Groeneveld, M. J., Boxhoorn, G., Kuipers, H. P. C. E., van Grinsven, P. F. A., Gierman, R., and Zuideveld, P. L., in "Proceedings, 9th International Congress on Catalysis, Calgary, 1988," p. 1743. Chemical Institute of Canada, Ottawa, 1988.
- Vogt, E. T. C., Van Dillen, A. J., Geus, J. W., and Janssen, F. J. J. G., *Catal. Today* **2**, 569 (1988).
- Baiker, A., Dollenmeier, P., Glinski, M., and Reller, A., *Appl. Catal.* **35**, 365 (1987).
- Ko, E. I., Chen, J. P., and Weissman, J. G., *J. Catal.* **105**, 511 (1987).
- Odenbrand, C. U. I., Andersson, L. A. H., Brandin, J. G. M., and Järås, S., *Catal. Today* **4**, 155 (1989).
- Berry, L. G., "Powder Diffraction File," Joint Committee on Powder Diffraction Standards, Philadelphia, 1967.
- Anderson, J. R., and Pratt, K. C., "Introduction to Characterization and Testing of Catalysts," 2nd ed., p. 64. Wiley, New York, 1974.
- Iler, R. K., "The Chemistry of Silica," p. 524. Wiley, New York, 1979.
- Bates, J. B., *J. Phys. Chem.* **57**, 4042 (1972).
- Etchepare, J., Meziaant, M., and Kaplan, P., *J. Chem. Phys.* **68**, 1531 (1978).
- Boccuti, M. R., Rao, K. M., Zecchina, A., Leonfanti, G. and Petrini, G., in "Proceedings, European Conference on Structure and Reactivity of Surfaces, Trieste, 1988" (C. Morterra, A. Zecchina, and G. Costa, Eds.). Stud. Surf. Sci. Catal., Vol. 48, p. 133, Elsevier, Amsterdam, 1989.
- McDevitt, N. T., and Baun, W. L., *Spectrochim. Acta* **20**, 799 (1964).
- Busca, G., Tittarelli, P., Tronconi, E., and Forzatti, P., *J. Solid State Chem.* **67**, 91 (1987).
- Peri, J. B., *J. Phys. Chem.* **70**, 2937 (1966).
- Hoffmann, P. and Knözinger, H., *Surf. Sci.* **188**, 181 (1987).
- Kondo, S., Yamagouchi, H., Kajiyama, Y., and Ishikawa, T., *J. Chem. Soc. Faraday Trans. 1* **80**, 2033 (1984).
- Tsyganenko, A. A., *Russ. J. Phys. Chem.* **56**, 1428 (1982).
- Busca, G., Saussey, H., Saur, O., Lavalley, J. C., and Lorenzelli, V., *Appl. Catal.* **14**, 245 (1985).
- Yates, D. J. C., *J. Phys. Chem.* **65**, 746 (1961).
- Ghiotti, G., Garrone, E., Morterra, C., and Bocuzzi, F., *J. Phys. Chem.* **83**, 2863 (1979).
- Ramis, G., Busca, G., and Lorenzelli, V., *J. Chem. Soc. Faraday Trans. 1* **83**, 1591 (1987).
- Morterra, C., Chiorino, A., Zecchina, A., and Fisticaro, E., *Gazz. Chim. Ital.* **109**, 683 (1979).
- Wagner, C. D., Passoja, D. E., Hillery, H. F., Kinisky, T. G., Six, H. A., Jansen, W. T., and Taylor, J. A., *J. Vac. Sci. Technol.* **21**, 33 (1982).
- Knözinger, H., and Ratnasamy, P., *Catal. Rev. Sci. Eng.* **17**, 31 (1978).
- Murata, M., Wakino, K., and Ikeda, S., *J. Electron Spectrosc. Relat. Phenom.* **6**, 459 (1975).